https://doi.org/10.5194/egusphere-2025-3522
Preprint. Discussion started: 14 October 2025

Investigating terrestrial water storage change in a western Canadian river basin with GRACE/GRACE-FO and fully-integrated groundwater – surface water modelling

Stephanie Bringeland[1], Steven K. Frey[2,3], Georgia Fotopoulos[1], John Crowley[4], Bruce Xu[2], Omar Khader[2], Hyung Eum[5], Babak Farjad[5], Andre R. Erler[2,6], Anil Gupta[5]

[1]Department of Geological Sciences and Geological Engineering, Queen's University, Kingston, Canada
[2]Aquanty Inc., Waterloo, Canada
[3]Department of Earth and Environmental Sciences, University of Waterloo, Waterloo, Canada
[4]Canadian Geodetic Survey, Surveyor General Branch, Natural Resources Canada, Ottawa, Canada
[5]Alberta Environment and Protected Areas, Calgary, Canada
[6]Department of Geography and Environmental Management, University of Waterloo, Waterloo, Canada

Correspondence to: Stephanie Bringeland (15smb14@queensu.ca)

Abstract. As hydrological trends shift in response to a warming climate, accurate characterization of hydrologic conditions and hydrologic change are imperative for water resources management, which is particularly important in the Canadian Prairies. In the study herein, a HydroGeoSphere (HGS) fully integrated groundwater – surface water (GW-SW) model is employed to evaluate trends and drivers of surface and subsurface water storage changes in the South Saskatchewan River Basin (SSRB). Terrestrial water storage anomalies (TWSA) derived from the Gravity Recovery and Climate Experiment (GRACE/GRACE-FO) are compared to HGS results; strong correlation is identified. The HGS solution facilitates decomposition of TWSA into constituent water storage components, namely surface water, soil moisture, and groundwater, and the GRACE/GRACE-FO solutions are used to validate the regional-scale TWSA and the interannual trends present in the SSRB TWSA time series. Meteorological and oceanic drivers and their impact on interannual hydrological trends in the SSRB are examined. Time-frequency analysis reveals a harmonic trend present in the SSRB TWSA with a period of 2.7-3.0 years, the inverse of which is present in the Oceanic Niño Index. The largest intra-annual water storage fluctuation is found in the soil profile, followed by snowpack, while groundwater experiences longer, multi-year cyclicity. Warmer oceanic conditions align with dry conditions in the SSRB and less snowpack, which leads to negative TWSA anomalies. Incorporating both high-resolution GW-SW models and regional-scale satellite gravimetry-derived estimates of TWSA facilitates a comprehensive analysis of hydrological dynamics in the Canadian Prairies and improved characterization of surface water and groundwater storage changes.

1 Introduction

The Canadian Prairies are home to diverse grasslands, wetlands, boreal forest, and extensive agriculture, containing over 80% of Canada's arable land (Veeman and Veeman, 2015). Climate change threatens to increase the likelihood and severity of

https://doi.org/10.5194/egusphere-2025-3522
Preprint. Discussion started: 14 October 2025

extreme weather events, and the gradual increase in average temperature is predicted to lead to increased evapotranspiration and rainfall and reduced snowpack throughout the prairie ecozone (Bonsal et al., 2013; Sauchyn et al., 2020; Tanzeeba and Gan, 2012). These changes to the hydrological dynamics of the Canadian Prairies will impact ecosystems and the sustainable management of water for urban, industry, and agricultural use (Wheater and Gober, 2013). As changing meteorological conditions impart demonstrable impact to water resources, the ability to model the complex interactions between different terrestrial water storage reservoirs (i.e. the land surface, soil profile, and groundwater system) becomes increasingly important. Further developing an accurate understanding and characterization of short- and long-term trends in regional hydrology is essential for preparing for the effects of climate change (Armour et al., 2013; Masson-Delmotte et al., 2021).

The South Saskatchewan River Basin (SSRB) spans from the eastern slopes of the Rocky Mountains to the confluence of the North and South Saskatchewan Rivers in central Saskatchewan and covers roughly 17% of the land area in Alberta. The basin is characterized by a semi-arid cold continental climate, with a large variation in temperature throughout the year (40°C to -40°C). The percentage of surface water usage that is attributed to agricultural use is 9% on average across all of Canada, but in the SSRB, agriculture accounts for 85% of all surface water usage (Martz et al., 2007). Reliance on groundwater is widespread especially among rural residences, and demand for groundwater could increase if a warming climate affects surface water availability (Sauchyn et al., 2020; Wheater and Gober, 2013). This study focuses on the portion of the SSRB located primarily within the province of Alberta (see the study region outlined in Fig. 1), including the Bow River Basin, the Red Deer River Basin, the Lower Saskatchewan River Basin, and the Oldman River Basin. Though the study excludes the Saskatchewan portion of the SSRB, the study area will be referred to as the SSRB for brevity.

https://doi.org/10.5194/egusphere-2025-3522
Preprint. Discussion started: 14 October 2025

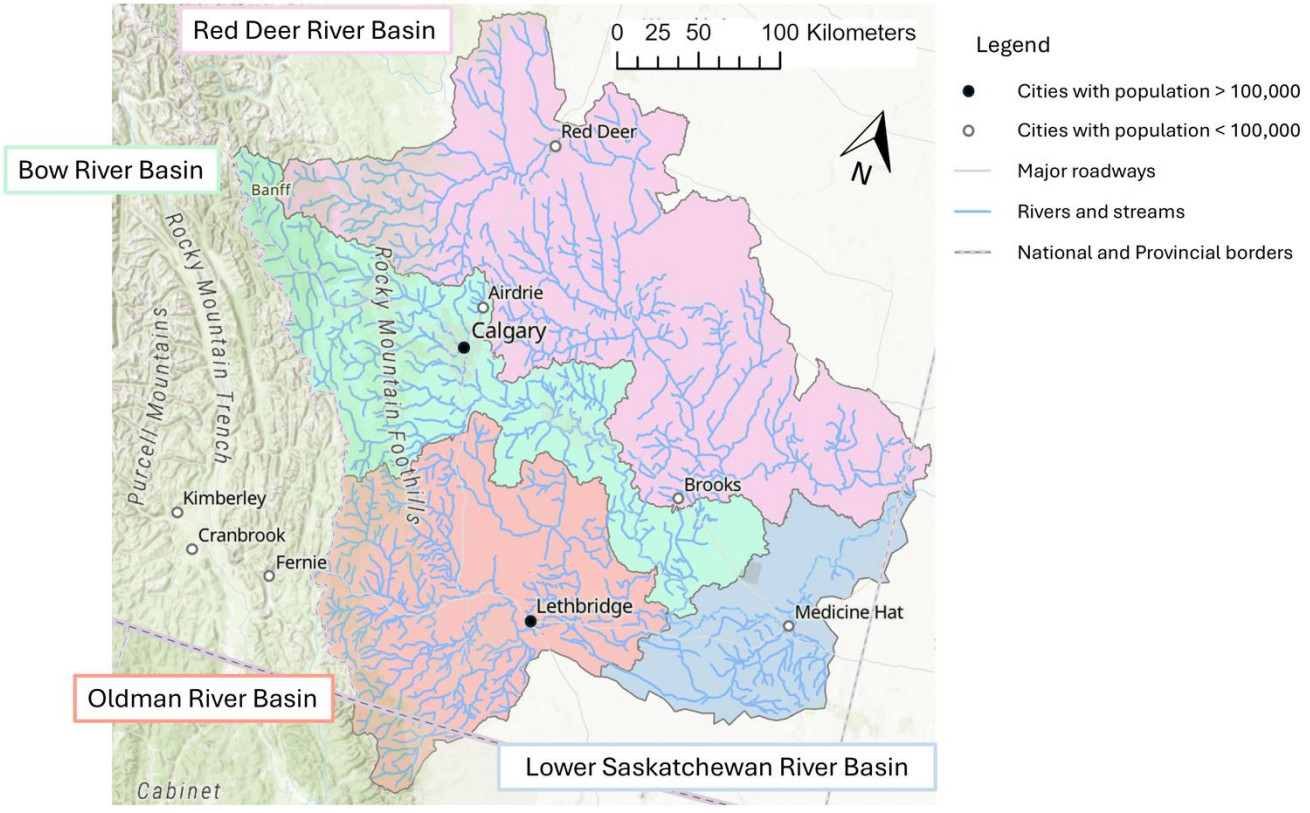

Figure 1: The Alberta portion of the South Saskatchewan River Basin and its major subbasins. Bow River Basin (green), Oldman River Basin (orange), Red Deer River Basin (pink), and the Lower Saskatchewan River Basin (blue).

The Gravity Recovery and Climate Experiment (GRACE, 2002-2017) and its follow-on mission (GRACE-FO, 2018 to present) have been used extensively to examine hydrological dynamics (Chen et al., 2009; Crowley et al., 2006; Tapley et al., 2019). GRACE/GRACE-FO provide consistent spatial coverage which is often unavailable via in-situ observations, especially in remote and sparsely inhabited regions. GRACE/GRACE-FO measurements are used to derive a monthly, vertically integrated (i.e., snow water equivalent, surface water, soil moisture, and groundwater) terrestrial water storage anomaly (TWSA). Observations from GRACE/GRACE-FO have been used to study event-scale drought and flooding (Abelen et al., 2015; Girotto et al., 2017; Scanlon et al., 2021) and long-term hydrological trends (Fatolazadeh and Goïta, 2021; Humphrey et al., 2016; Scanlon et al., 2018). Hydrological models are used in conjunction with GRACE/GRACE-FO to isolate particular components of terrestrial water storage such as groundwater (Famiglietti et al., 2011), or to examine drivers of terrestrial water storage change, such as irrigation (Scanlon et al., 2021). Hamdi et al. (2025) combines GRACE/GRACE-FO data with remotely sensed precipitation, evapotranspiration, soil moisture, runoff, and snow thickness, using a machine learning

https://doi.org/10.5194/egusphere-2025-3522
Preprint. Discussion started: 14 October 2025

approach to estimate groundwater storage in the Saskatchewan River Basin, though does not consider spatial variability within the basin.

To examine water storage variability in the SSRB, this study employs a HydroGeoSphere (HGS; Aquanty, 2024) fully integrated groundwater – surface water (GW-SW) model in conjunction with estimates of TWSA derived from the Gravity Recovery and Climate Experiment (GRACE) and its follow-on mission (GRACE-FO), which have been used extensively to examine hydrological dynamics (Chen et al., 2009; Crowley et al., 2006; Tapley et al., 2019). An additional TWSA model, namely the Global Land Data Assimilation System (GLDAS) Catchment Land Surface Model (CLSM; Li et al., 2020; Rodell et al., 2004), was included for comparison. Combining hydrologic model-based estimates of water storage with dedicated satellite gravity observations allows for the independent validation of model results, and the high-resolution HGS model, which integrates surface and subsurface flow regimes, allows for the decomposition of the regional TWSA into individual storage components, including surface water, soil moisture, and shallow and deep groundwater.

The main objectives of this study are to (i) compare satellite gravity-derived terrestrial water storage anomalies with hydrologic model-derived terrestrial water storage anomalies in the SSRB over a period of 17 years, (ii) decompose the satellite gravity-derived TWSA into water storage components using the model-derived TWSA and assess the time-variable frequency content of each water storage component, and (iii) assess climatological drivers of hydrologic trends in the SSRB based on a time-frequency analysis of the TWSA.

Section 2.0 provides a detailed description of the data and pre-processing steps used in the analysis and is followed by the presentation and discussion of study results in Sect. 3.0. Section 4.0 provides key conclusions and an outlook for future work.

2 Description of Data

2.1 GRACE/GRACE-FO

The GRACE and GRACE-FO (henceforth ‘GRACE’) data used in the analysis are derived from the Jet Propulsion Laboratory (JPL) monthly global mascon solutions (RL06.1M.MSCNv03) and extend from April 2002 to December 2019, which is the end of the HGS simulation interval. The JPL mascons are provided on a 0.5°×0.5° grid, but derived from native 3° equal-area spherical caps placed on an elliptical Earth (Landerer et al., 2020; Watkins et al., 2015; Wiese et al., 2016, 2023). Included in the JPL mascon solutions is a correction for glacial isostatic adjustment (GIA) based on the ICE6G_D (VM5a) model from Peltier et al. (2018). The JPL mascon data represents TWSA in cm equivalent water height (EWH) with respect to a January 2004 to December 2009 baseline. This baseline period is referred to as the ‘GRACE baseline’ and is used throughout the analysis to ensure consistent comparison of datasets. Gaps in the GRACE/GRACE-FO data record in between the two missions (11 consecutive months) and within the missions (22 months) have been filled using a machine learning technique described in Bringeland and Fotopoulos (2024) for continuous comparison. The JPL mascons were ultimately used in the analysis, although the Centre for Space Research mascon solutions were also considered, and were found very similar to the JPL mascon solutions (Save, 2020; Save et al., 2016). The JPL mascons (henceforth ‘JPL-M’) were spatially averaged to the study domain

https://doi.org/10.5194/egusphere-2025-3522
Preprint. Discussion started: 14 October 2025

using a 0.5°×0.5° gridded mask generated using basin boundaries based on Alberta Watersheds 2011 (https://geospatial.alberta.ca/titan/rest/services/environment/alberta_watersheds/MapServer; last accessed April 07, 2025).

In addition to the JPL GRACE mascon solution, the GRACE solution produced by the Canadian Geodetic Survey (CGS) is also utilized. For brevity, this approach is referred to as the CGS method. This method incorporates the GRACE and GRACE-FO Level 2 spherical harmonic coefficient (SHC) solutions from the University of Texas Center for Space Research (CSR GRACE RL06 and GRACE-FO RL06.3) and applies a series of corrections and filtering steps to enhance signal quality while removing unwanted noise. Unlike mascon solutions, which impose predefined spatial constraints and model-based regularizations, the CGS approach provides greater processing flexibility while preserving the full range of geophysical and hydrological signals. One of its key advantages is the ability to define analysis regions based on hydrological boundaries, ensuring a more accurate representation of regional TWSA. In contrast, mascon solutions rely on a fixed grid-based structure (typically 0.25°–0.5° spacing but with a true native resolution closer to 3°), which can lead to spatial leakage and inaccuracies near hydrologically complex regions. The CGS method overcomes this limitation by using spherical harmonic convolution and precise user-defined regions that can be aligned with watershed boundaries.

In the CGS method, missing degree-1 harmonics are replaced using externally derived estimates from GRACE Technical Note 13 (TN-13) (Sun et al., 2016; Swenson et al., 2008), while the C2,0 coefficient—which represents Earth's oblateness—is corrected using Satellite Laser Ranging (SLR) data (Loomis et al., 2019). To maintain consistency with other GRACE-derived estimates, GIA corrections are applied using the ICE-6G_D (VM5a) GIA model (Peltier et al., 2015, 2018), the same model used for JPL data processing. To further improve the accuracy of the SHC solutions, the destriping method of Crowley and Huang (2020) is applied to remove correlated errors, while a statistical filtering approach (Davis et al., 2008) eliminates high-degree spherical harmonic coefficients that lack statistically significant trends or seasonal signals. To suppress high-frequency noise for SHCs with statistically significant signal, a 167 km half-width (~1.5°) Gaussian smoothing filter is applied (see Crowley et al., 2006). Spherical harmonic coefficients are converted from geoid height change to mass change, following the (Wahr et al., 1998) methodology. Finally, regional mass variations are then extracted using spherical harmonic convolution, integrating mass change estimates over the defined study area (see Crowley et al., 2006). The final product is a monthly time series of TWSA, capturing both seasonal fluctuations and long-term trends in water storage.

2.2 HydroGeoSphere (HGS)

The HGS model is a fully integrated GW-SW model that has been used extensively in Canadian hydrological analysis, including in the Athabasca River Basin north of the SSRB (Hwang et al., 2023) and the Northern Great Plains (Frey et al., 2021). The HGS model used in this study implicitly couples three governing equations, namely the three-dimensional Richards equation for variably saturated subsurface flow, the two-dimensional diffusion wave equation for overland flow, and the Manning's open channel flow equation for one-dimensional river flow, which are described more completely in Frey et al. (2021) and Aquanty (2024). Water exchange between the three domains occurs dynamically in response to hydraulic gradients

https://doi.org/10.5194/egusphere-2025-3522
Preprint. Discussion started: 14 October 2025

that vary spatially and temporally across the domain. The HGS numerical solution utilizes a control volume finite element approach with adaptive time-stepping and OpenMP parallelization (Hwang et al., 2014).

The basis of the HGS model is an unstructured three-dimensional finite element mesh, which in the case of the SSRB model is composed of 11 subsurface layers and one surface layer, 2.5 km maximum node spacing away from river features, and 2 km maximum node spacing along river features. On each of the mesh sheets (surfaces) there are 51,279 nodes which form 101,214 finite element per model layer. In total, over the 13 mesh sheets and 12 mesh layers, there are a respective 666,627 nodes and 1,214,568 elements. In the one-dimensional channel domain, there are 14,125 km of discretely resolved Strahler order 3+ rivers.

The three-dimensional structure of the model is presented in Fig. 2a. Topography is defined by a 15 m resolution, LiDAR-based digital elevation model provided by Alberta Environment and Protected Areas (AEPA). Landcover distribution on the land surface of the model is represented with 2015 North America Land Change Monitoring System 30 m resolution data (Latifovic et al., 2012). The top three subsurface layers are positioned at 0.25 m, 0.5 m, and 1 m fixed depth from surface and represent spatially varying soil textures derived from Soil Landscapes of Canada (Soil Landscapes of Canada Working Group, 2010). Beneath the soil layers are two Quaternary geology layers, based on material distribution defined by the Surficial Geology of Canada map-based dataset (Geological Survey of Canada, 2014) that extend down to top of bedrock. The lower six layers are derived from a simplified version of the 3D Provincial Geological Framework Model of Alberta, Version 2 (Alberta Geological Survey, 2019). Across the soil, Quaternary, and bedrock layers there are a total of 740 different porous media material zones configured into the model.

Forcing data, which includes liquid water flux (LWF) and potential evapotranspiration (PET), for the HGS simulation was derived from 0.1 ° (~10km) resolution, daily transient Alberta hybrid climate data (Eum and Gupta, 2019). PET was calculated using a simplified Priestley-Taylor method that requires only precipitation and temperature (Alberta Agriculture and Rural Development, 2013) while LWF was obtained from the sum of rainfall and snowmelt, with the later calculated using a process-based snow model (Kienzle 2008; Walter et al., 2005), modified by incorporating a S-curve approach (Kienzle, 2008) to consider diurnal temperature in a day, forced by the Alberta hybrid climate data.

For the purpose of this study, HGS model performance validation is based on 2002 – 2015 weekly transient naturalized river flow rates at four strategically positioned gauges that capture flows from each of the three major subbasins and at the SSRB outlet, and average groundwater levels at 79 observation wells (Fig. 2b). Simulated groundwater levels show a strong correlation to measured levels (Fig. 2c), and simulated surface water flow rates align well with estimated naturalized flow data (Fig. 2d) based on both the Nash-Sutcliffe model efficiency coefficient (NSE) and percent bias (PBias) (Moriasi et al., 2007).

https://doi.org/10.5194/egusphere-2025-3522
Preprint. Discussion started: 14 October 2025

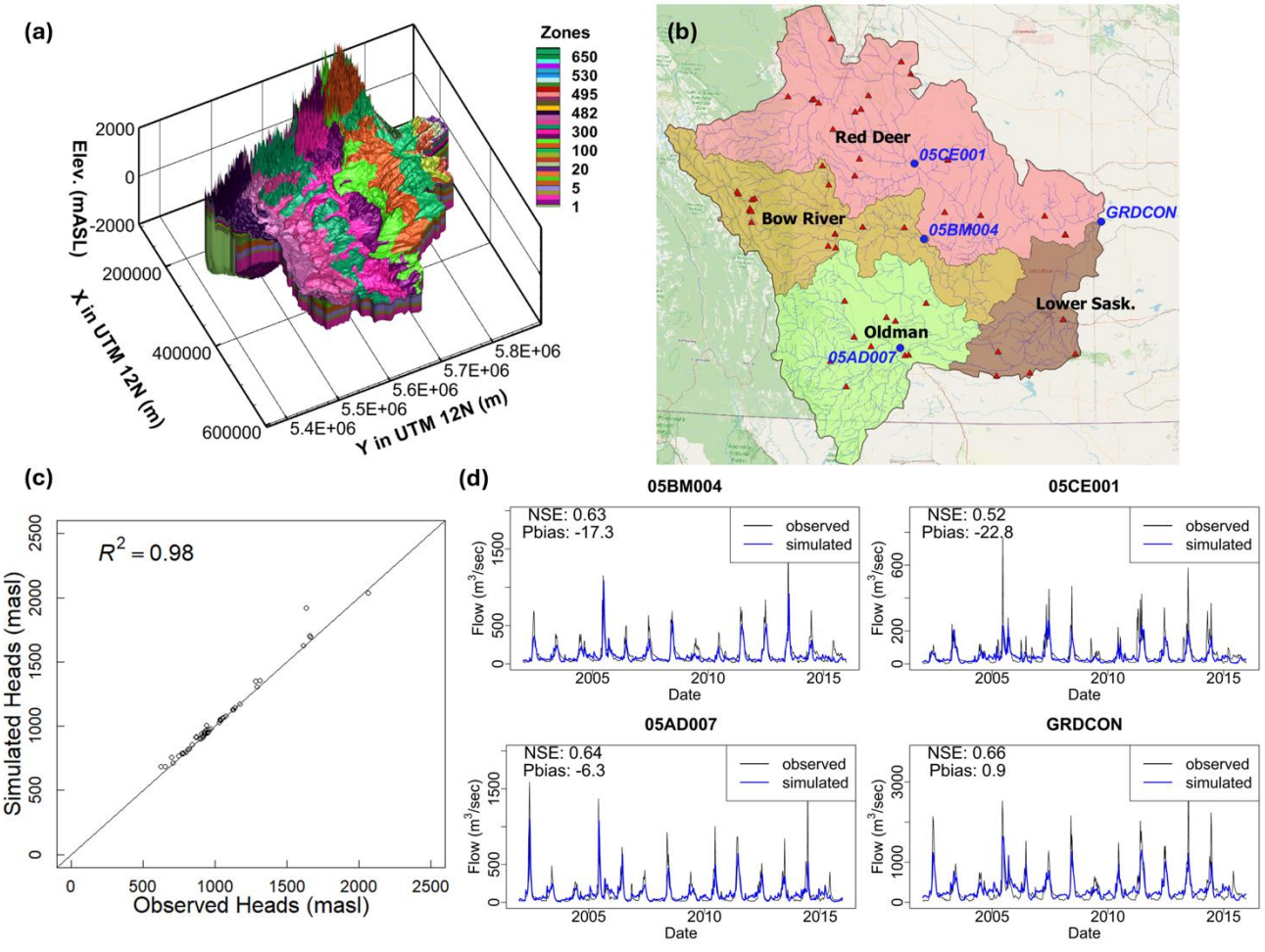

Figure 2. (a) Three-dimensional isometric perspective of the HydroGeoSphere SSRB model and its subsurface porous media zonation, (b) hydrometric gauging station locations in the Red Deer, Bow River, and Oldman River subbasins, and at the SSRB outlet, and groundwater monitoring point (triangle markers) locations across the SSRB, (c) groundwater level simulation performance, and (d) surface water simulation performance at the four hydrometric station locations.

For comparison against GRACE TWSA data, HGS water storage changes in the surface domain, 0 – 1 m soil profile, and the groundwater system required averaging to monthly temporal increments and conversion to an anomaly value. The individual components of the HGS output were summed and then converted to EWH by dividing by the area of the SSRB. To produce an anomaly from the HGS data, the mean was removed and then the cumulative sum of the monthly anomalies was calculated. Finally, the snow water equivalent (SWE) was added, and the mean with respect to the GRACE baseline was removed, resulting in the HGS TWSA time series comparable to that of GRACE. The same process was applied to each of the storage components.

https://doi.org/10.5194/egusphere-2025-3522
Preprint. Discussion started: 14 October 2025

2.3 Catchment Land Surface Model

The Catchment Land Surface Model (CLSM) from the NASA Global Land Data Assimilation System (GLDAS; Rodell et al., 2004) was used to provide an additional comparison for TWSA in the study area. GLDAS is an uncoupled land surface modelling system that incorporates satellite and terrestrially acquired data to produce a suite of hydrometeorological variables at a global scale. The CLSM V2.1 dataset used herein is provided on a 1.0°×1.0° grid as a monthly averaged product (Li et al., 2020). The instantaneous terrestrial water storage ('TWS_inst') variable was used in this analysis, spatially averaged within the study area and presented in cm EWH. The GRACE baseline was removed to ensure consistent comparison between datasets.

2.4 Oceanic Indices

Relationships between TWSA and several indices representing historical oceanic conditions were considered, namely the Oceanic Niño Index (ONI), the North Atlantic Oscillation (NAO), and the Pacific Decadal Oscillation (PDO). The ONI represents the 3-month average sea surface temperature (SST) anomaly of the east-central tropical Pacific from 120°W to 170°W. An ONI anomaly greater than +0.5°C represents El Niño conditions, while an ONI anomaly less than -0.5°C represents La Niña conditions (NOAA, 2019). The ONI is closely related to the PDO, an index which is computed using the extended reconstruction of SSTs produced by the National Oceanic and Atmospheric Administration (NOAA) and the Mantua PDO index (Huang et al., 2017; Mantua and Hare, 2002; Newman et al., 2016). The warm phases of the ONI and PDO are linked to warmer, drier conditions in the Canadian Prairies (McCabe and Dettinger, 2002; Shabbar et al., 2011). The NAO index represents the anomalies in the surface sea-level pressure difference between the Subtropical High and the Subpolar Low in the Atlantic (Hurrell and Deser, 2010). There does not appear to be a significant correlation between the NAO index and the hydrology of the Canadian Prairies, but this index is included in the analysis to ensure a comprehensive examination of possible drivers of hydrological trends in the SSRB (Chartrand and Pausata, 2020; Wittrock and Ripley, 1999).

3 Results and Discussion

3.1 Terrestrial water storage anomalies

Figure 3 shows the HGS, GLDAS CLSM, and GRACE-derived (JPL and CGS) terrestrial water storage anomalies for the SSRB throughout the study period. The seasonal peaks in TWSA occur immediately prior to the spring thaw, in April/May, with the seasonal low coinciding with the end of summer, August/September.

https://doi.org/10.5194/egusphere-2025-3522
Preprint. Discussion started: 14 October 2025

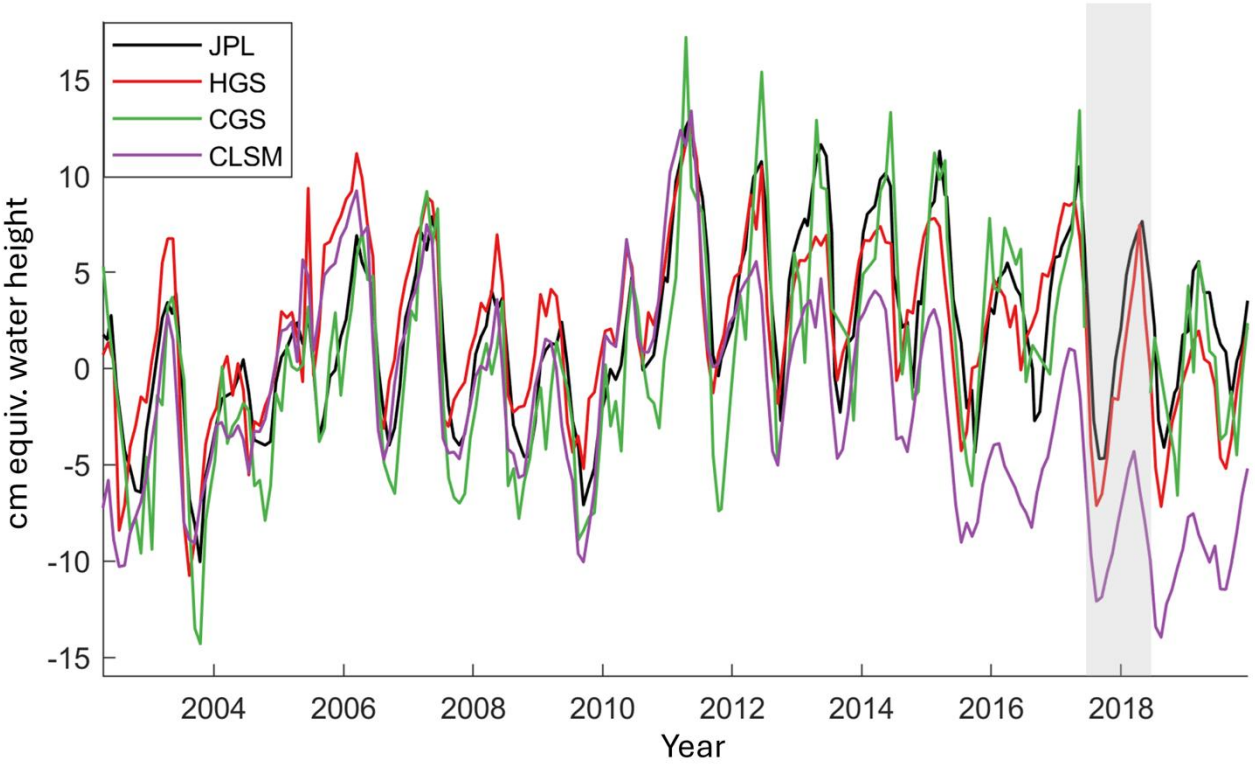

Figure 3: Terrestrial water storage anomalies in the SSRB derived from HydroGeosphere (HGS, red), JPL GRACE/GRACE-FO mascon solutions (JPL, black), CGS GRACE/GRACE-FO solutions (CGS, green), and the GLDAS CLSM product (CLSM, purple). Shading indicates gap between GRACE and GRACE-FO missions.

The HGS TWSA values approximately align with the GRACE-derived April/May peaks but overestimate late summer TWSA relative to GRACE. The CLSM TWSA increasingly underestimates TWSA relative to HGS, JPL, and CGS TWSA, especially after 2012. All four of the TWSA time series were decomposed into their annual, linear, and residual trends, which are shown in Fig. 4. Signal decomposition (separation into annual, long-term, and residual trends) was done using least-squares regression to fit and remove a 31.7 nHz (1-year period) harmonic trend to the data, followed by a fit to remove the long-term trend.

https://doi.org/10.5194/egusphere-2025-3522
Preprint. Discussion started: 14 October 2025

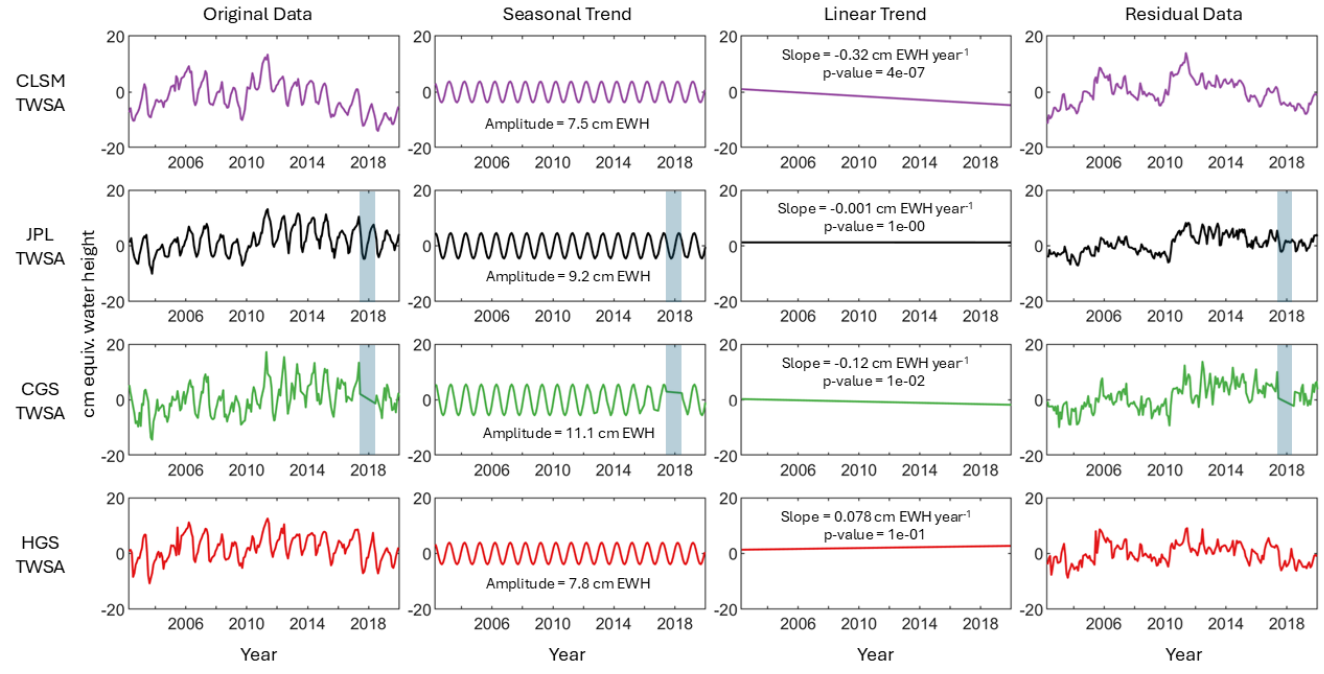

Figure 4: Signal decomposition of terrestrial water storage anomalies from the GLDAS CLSM product, JPL GRACE/GRACE-FO mascon solutions, CGS GRACE/GRACE-FO solutions, and HydroGeoSphere. Shading indicates gap between GRACE and GRACE-FO missions.

The GRACE-derived (JPL and CGS) time series have a larger seasonal amplitude (9.2 cm EWH and 11.1 cm EWH, respectively) than the model-derived time series (HGS and CLSM, 7.8 and 7.5 cm EWH, respectively). The linear trend of the HGS time series is slightly positive, which differs from the slightly negative linear trends of the CGS and JPL TWSA time series. The method used to calculate the HGS TWSA values, which involves taking the cumulative sum of the anomalies in water storage, may contribute to this discrepancy, as the overestimation of any anomaly would be amplified throughout the study period. Results show that HGS TWSA overestimates late summer TWSA relative to JPL or CGS. The processing method used to convert the HGS output to TWSA values comparable with GRACE involves taking a cumulative sum; the positive bias in the summer months thus contributes to the aforementioned positive linear trend which may not be reflected in the GRACE-derived TWSA. The CGS TWSA has a slight statistically significant ($p = 0.01$) negative trend, though it is smaller in magnitude than the significant negative linear trend present in the CLSM TWSA. As HGS TWSA matches the GRACE-derived TWSA more closely than CLSM TWSA, the CLSM will be omitted from the rest of the analysis.

The interannual trends evident in the residual values in Fig. 4 (rightmost column) are similar throughout the different derivations of TWSA. The beginning (2002-2006) of the time series reflects the recovery from the 1999-2004 drought that affected the Canadian Prairie provinces (Bonsal and Regier, 2007) and is followed by a negative trend leading to the 2008-

https://doi.org/10.5194/egusphere-2025-3522
Preprint. Discussion started: 14 October 2025

2010 drought (Sauchyn et al., 2020). Relatively wet conditions follow after 2010 until 2012, at which point a gradual decline in TWSA ultimately leads to drought in spring/summer 2019 (Sauchyn et al., 2020).

3.2 Time-variable frequency of water storage

The HGS TWSA, decomposed into constituent storage components, are shown in Fig. 5(a), (b), and (c), while Fig. 5(d) shows the SWE storage in the SSRB with the GRACE baseline mean removed (i.e., shown as an anomaly).

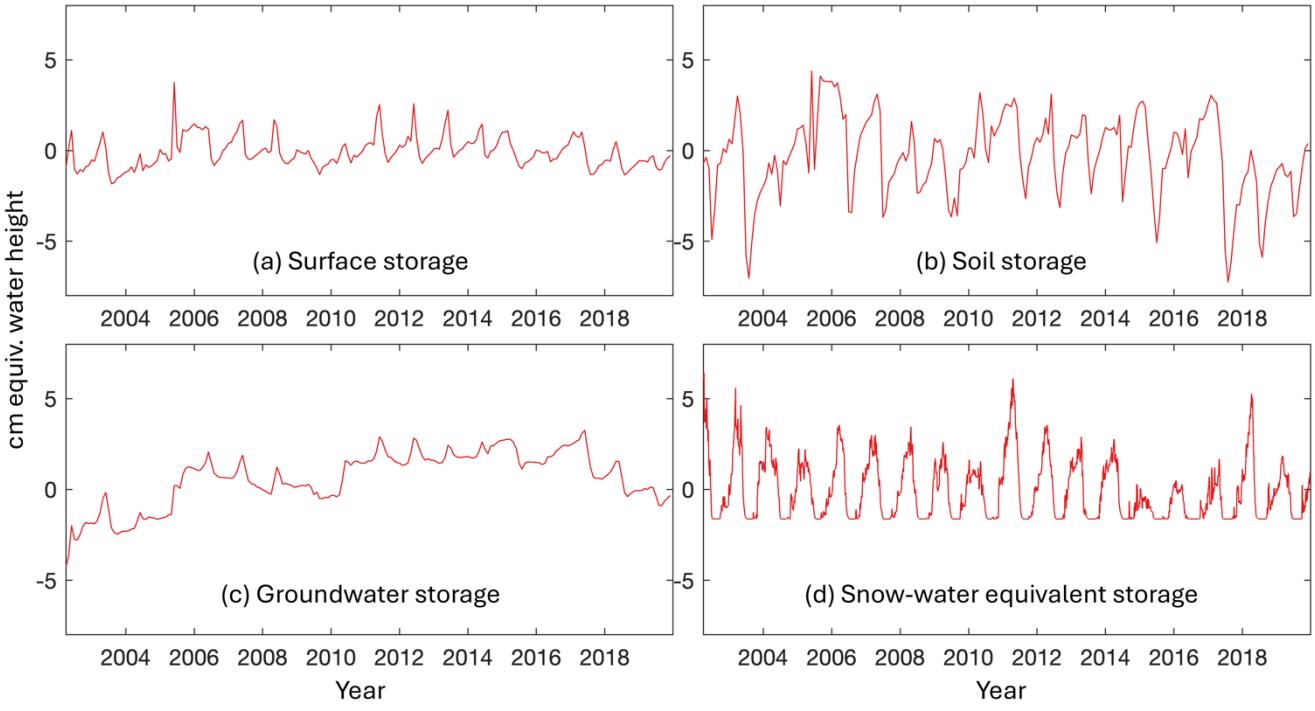

Figure 5: Cumulative HGS-based anomalies for (a) surface water storage, (b) soil moisture storage, and (c) groundwater storage, centred around the mean of the GRACE/GRACE-FO baseline period (Jan. 2004 – Dec. 2009). (d) Snow-water equivalent storage is presented as an anomaly with respect to the same baseline but is not cumulated over the availability period.

Soil storage in the SSRB shows the highest variability of any storage component, impacted both by seasonal variation and interannual trends. The SWE storage owes most of its variability to a seasonal fluctuation, but interannual differences in the amount of SWE storage are evident. The groundwater storage is the most 'dampened' of any storage component, with a clear interannual trend and a low amplitude seasonal variation. Tangdamrongsub et al. (2021) had similar results (lower frequency, 'dampened' trends in groundwater compared to soil moisture storage) when using a priori hydrological data to separate GRACE-derived TWSA into water storage components globally. The storage components are shown in a stacked bar chart in Fig. 6.

https://doi.org/10.5194/egusphere-2025-3522
Preprint. Discussion started: 14 October 2025

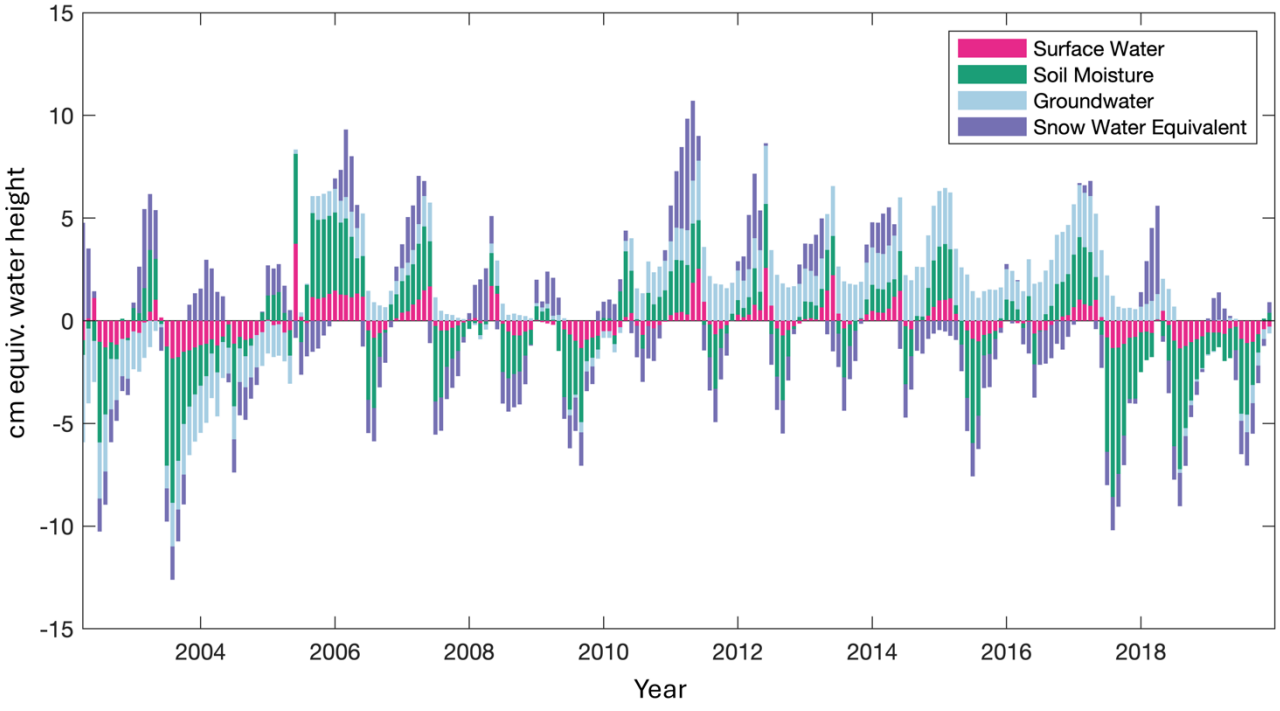

Figure 6: Stacked bar plot showing the monthly anomalies for different water storage components in the SSRB, including surface water (pink), soil moisture (green), groundwater (light blue), and snow-water equivalent (purple).

The separation of TWSA into its components allows for a higher resolution analysis of water storage dynamics than is possible with GRACE/GRACE-FO alone. This separation can allow for detailed analysis of agricultural or meteorological drought within different components of the water storage system and how pre-existing conditions may contribute to the vulnerability of an area to drought or flooding events. For example, the catastrophic flooding events of 2013 in southern Alberta may have been worsened by the positive groundwater anomalies (see Fig. 5) in the years leading up to the disaster, as excess runoff from heavy rainfall could not be offset by infiltration (Pomeroy et al., 2016). The largest proportion of the TWSA in the SSRB tends to be attributed to soil moisture storage, which is particularly apparent during times of drought (e.g., 2003, 2017, Fig. 5). Analysis of precursor conditions to extreme events can allow for better prediction and preparedness (Davitt et al., 2019). Climate change projections suggest that the Canadian Prairie region will be more prone to drought as temperatures rise, though increased precipitation is expected to increase groundwater recharge (Berg and Sheffield, 2018; Wheater and Gober, 2013; Zhang et al., 2020).

A continuous wavelet transform using the analytic Morse wavelet is used to assess the time-frequency content of the TWSA data (Lilly and Olhede, 2009, 2012). The Lomb-Scargle power spectral density estimates are used to show the dominant frequencies present in the data (Lomb, 1976; Scargle, 1982). As the continuous wavelet transform requires equally spaced data, the gaps in the CGS TWSA data were filled using a simple time series decomposition technique. The annual signal and linear trend (see Fig. 4) were calculated on a monthly interval. The gaps in the residual values were linearly interpolated at the

https://doi.org/10.5194/egusphere-2025-3522
Preprint. Discussion started: 14 October 2025

same monthly interval. The sum of the annual, linear, and residual components resulted in the complete CGS TWSA time series. This data product was used for the continuous wavelet transform, as the Lomb-Scargle power spectral density estimates do not require evenly spaced data. The time-frequency content of the JPL TWSA, CGS TWSA, HGS TWSA, and HGS surface water, soil moisture, and groundwater are shown in Fig. 7.

The power spectral density values in the Lomb-Scargle periodograms as well as the continuous wavelet transform amplitudes are normalized to the range of each individual parameter (Fig. 7).

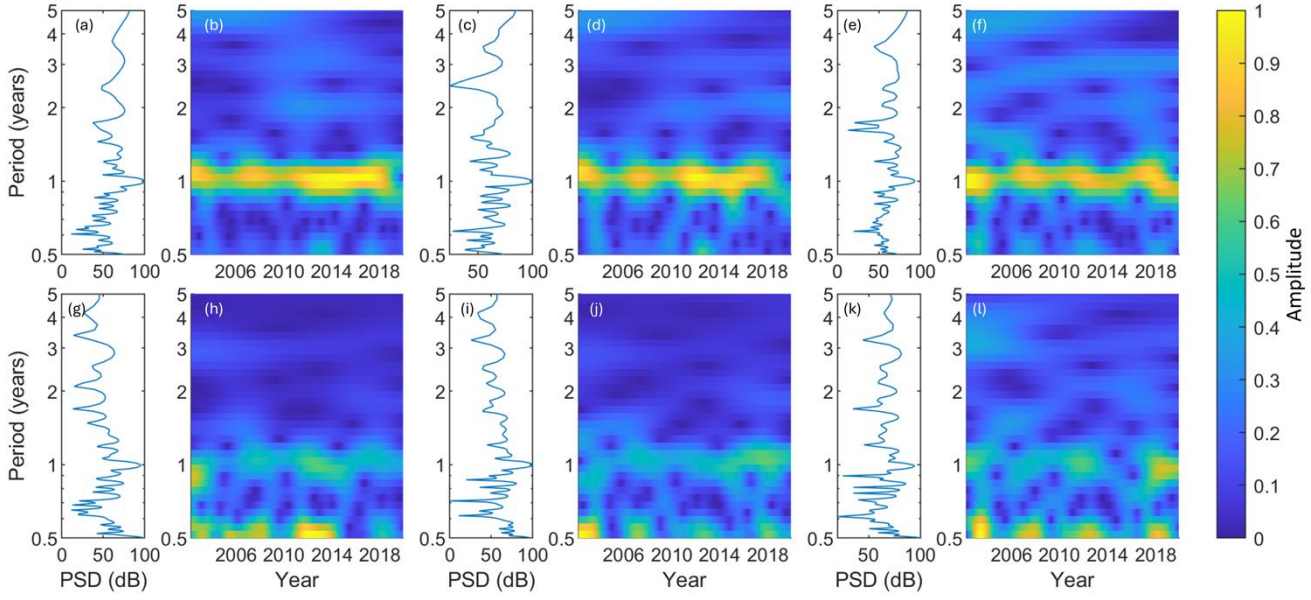

Figure 7: Lomb-Scargle periodograms (power spectral density (PSD), left) and continuous wavelet transforms (right) of the JPL TWSA (a, b), CGS TWSA (c, d), HydroGeoSphere TWSA (e, f), HydroGeoSphere surface water (g, h), HydroGeoSphere soil moisture (i, j), and HydroGeoSphere groundwater (k, l). Amplitude and PSD have been scaled from 0-1 and 0-100, respectively.

The annual signal (period = 1 year) is the most prominent in all 6 parameters, though the period is inconsistent throughout the time series (Fig. 7(d)). The JPL, CGS, and HGS TWSA all observe a peak in the amplitude of the annual signal around 2007, and again between 2010 and the end of 2017. The CGS and HGS TWSA show a more detailed fluctuation in the period of the annual signal between 2010 and 2017, where the annual signal is slightly longer than one year around 2012, slightly shorter than one year around 2014, and peaking at around 1.1 years between 2016 and 2017. The TWSA time series (Fig. 7(a-f)) contain interannual frequency trends with periods between 2-4 years, as is shown in the Lomb-Scargle periodograms (Fig. 7(a), (c), and (e)). The HGS storage components show similar power spectral density (PSD) peaks with periods between 2-3 years. The groundwater storage component shows a higher PSD in this range (Fig. 7(k), 82 dB peak at period = 2.8 years) than

https://doi.org/10.5194/egusphere-2025-3522
Preprint. Discussion started: 14 October 2025

the soil moisture and surface water components, which suggests that the interannual TWSA trends are more attributable to slow fluctuations in groundwater storage in the SSRB. None of the storage components have as strong an annual signal as the TWSA time series; the seasonal SWE trends likely contribute significantly to this frequency band.

3.3 Drivers of water storage change

To investigate relationships between prominent drivers of hydrological change and individual water storage components, the average annual anomaly for each driver (precipitation, evapotranspiration) and for each water storage component (surface water, soil moisture, groundwater, and SWE) was calculated to remove seasonal effects. Precipitation in this case refers to liquid water flux (rainfall + snowmelt), and evapotranspiration represents the simulated actual evapotranspiration; both parameters were generated as output variables by the HydroGeoSphere model. Plots showing the hydrological driver anomalies and water storage anomalies are presented in Fig. 8. Relationships between each pair of variables are modelled with a best fit line (red) and the upper and lower 90% confidence bounds are shown (green).

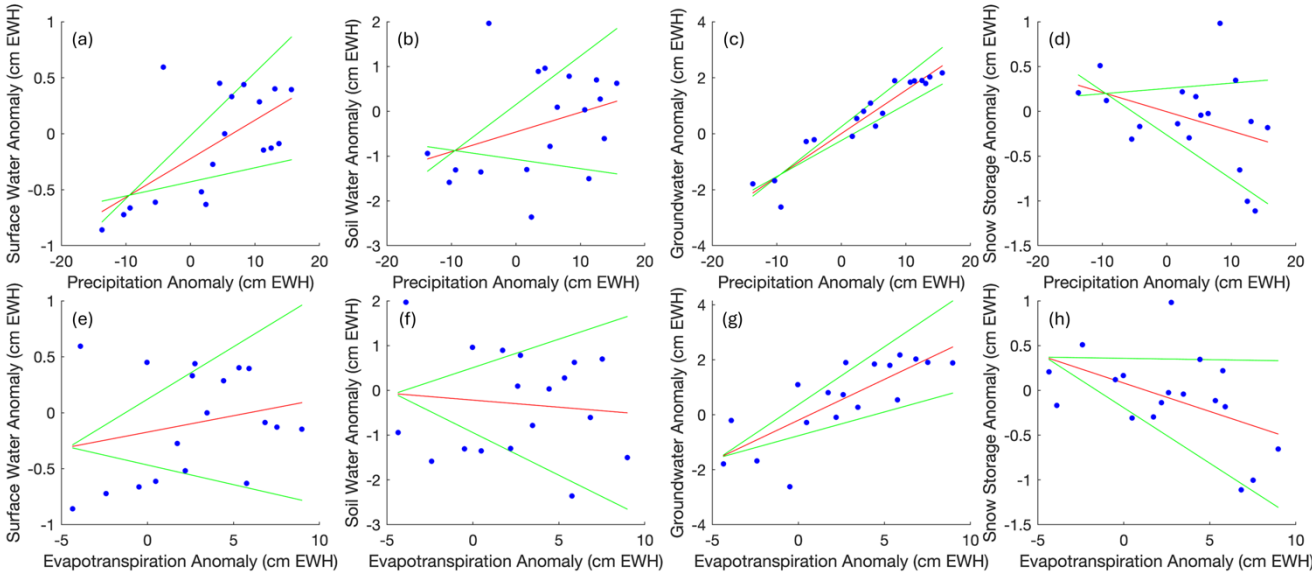

Figure 8: Annual anomaly (cm equivalent water height) in four components of water storage, namely surface water (a, e), soil storage (b, f), groundwater (c, g), and snow water equivalent (d, h), as a function of the annual anomaly in two drivers of hydrological change, precipitation (a-d) and actual evapotranspiration (e-h). Linear trends (red) and the respective 95% confidence intervals (green).

Some of the relationships between variables are straightforward and expected; anomalously high precipitation leads to anomalously high surface water and groundwater (Fig. 8(a), (c)). However, the relationships between evapotranspiration and surface water and soil moisture are more complex. In this analysis, evapotranspiration is considered the 'driving' variable, but positive anomalies in surface water and soil moisture imply more water is available to vegetation, and thus, more water can be

https://doi.org/10.5194/egusphere-2025-3522
Preprint. Discussion started: 14 October 2025

transpired, leading to a positive evapotranspiration anomaly. In this scenario, the surface and soil water components act as an independent variable driving evapotranspiration. Conversely, evapotranspiration anomalies can represent other meteorological anomalies such as temperature and latent heat flux, which should cause a negative anomaly in surface and soil water when increased. This complex relationship accounts for the wider confidence bounds shown in Figs. 8(e) and (f). It is projected that evapotranspiration will increase in the Canadian Prairies as a result of a warming climate, which may affect the availability of surface water and soil moisture (Eum et al., 2017; Sauchyn et al., 2020). The increase in precipitation associated with the projection of increased temperatures may offset this increase in evaporation and evapotranspiration, as is discussed by Roderick et al. (2015), referred to as the 'aridity paradox'; the conflicting trends of increasing potential evapotranspiration and increasing precipitation with increasing temperature, and whether a warmer climate leads to more or less aridity. Spence et al. (2022) project up to an 11% decrease in maximum annual SWE per °C of warming in the grassland basins of the Canadian Prairies, which cover much of the SSRB within Alberta (He et al., 2023). Decreasing snowpack may reduce the amplitude of the annual signal in the TWSA (see Fig. 8), increasing the relative dominance of interannual trends in the SSRB. The trend of 'wetter winters', that is, a shortening snow season and lengthening rain season, is observed and projected in the Canadian Prairies as average temperatures increase due to climate change (Dumanski et al., 2015; Sauchyn et al., 2020).

Of all of the oceanic indices considered in this study, the Oceanic Niño Index exhibits the strongest correlation with TWSA in the SSRB. To remove seasonal impacts and assess only the interannual trends, the HGS TWSA residuals (annual and linear trends removed) were smoothed using a 6-month moving average and were compared to the ONI. The results are shown in Fig. 9, along with the frequency content (Lomb-Scargle periodograms) of each of the ONI (right) and smoothed HGS residual TWSA (left). The ONI axis (right) has been reversed.

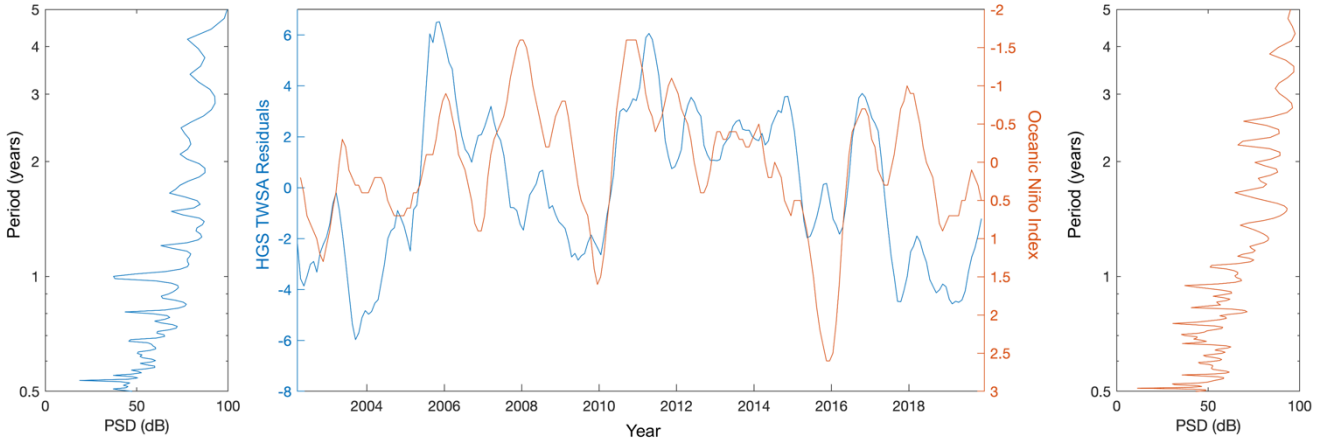

Figure 9: The Oceanic Niño Index (middle, orange) with the residual values (seasonal signal removed) of the HydroGeoSphere TWSA (middle, blue) in the study domain, smoothed using a 6-month moving mean. Note that the right y-axis in the centre plot is flipped. Lomb-Scargle periodograms of the smoothed HydroGeoSphere TWSA residuals (left, blue) and the ONI (right, orange).

https://doi.org/10.5194/egusphere-2025-3522
Preprint. Discussion started: 14 October 2025

The ONI has a moderate negative correlation (correlation coefficient = -0.38) with the smoothed HGS residual TWSA in the SSRB. This is consistent with McCabe and Dettinger (2002), Asong et al. (2018), and Shabbar et al. (2011) which suggest that a positive ONI anomaly is related to warm, dry conditions in the Canadian Prairies. The Lomb-Scargle periodograms of both parameters show a peak around the 2.7-3.0-year period (Fig. 7). This correlation explains some, but not all, of the interannual variability of TWSA in the SSRB. The El Niño Southern Oscillation (ENSO) has changed and is projected to continue to change temporally, with multi-year ENSO events becoming more frequent (Lu et al., 2025). Prolonged warm-phase ENSO events, linked with dry conditions in the SSRB, could increase the length and severity of drought. The characteristics of ENSO events are also projected to change in terms of location of the maximum sea surface temperature anomalies, with central Pacific El Niño events increasing with respect to eastern Pacific El Niño events (Yeh et al., 2009). It is unclear what effect this will have on the TWSA of the SSRB.

4 Conclusions and Future Outlook

Integrating both satellite gravimetry and high-resolution fully integrated GW-SW models allows for a comprehensive examination of water storage dynamics in the Canadian Prairies. Comparing GRACE- and model-derived TWSA reveals a possible 15-32% underestimation of the seasonal amplitude in the HGS model and the GLDAS CLSM model, but the HGS model more closely matched the interannual trends present in the GRACE-derived TWSA. These interannual trends in the SSRB reflect large-scale events such as the 2008-2010 drought that was observed throughout the Canadian Prairies (Sauchyn et al., 2020). Decomposing TWSA into its constituent storage components using HGS allows for an examination of the influence of short- and long-term drought or flooding events on different water storage domains. This decomposition can provide insight into hydrological conditions that increase vulnerability to drought or flooding events, given anomalous meteorological events. Surface and groundwater are essential for agricultural and human activities in the SSRB and understanding the interannual and seasonal dynamics is imperative for sustainable water management, especially as climate change increases the likelihood and severity of extreme weather events. Understanding projected climate conditions and their relationships to components of water storage, such as snow water equivalent or groundwater, can help make sustainable water management strategies more robust.

Assessing the time-frequency content of components of water storage reveals an interannual harmonic trend with a 2–4-year period which is more prominent in the groundwater component of TWSA than surface water storage or soil moisture. This is likely related to global-scale oceanic and meteorological cyclicity which affects the average temperature and amount of precipitation, and thus groundwater recharge, present in the Canadian Prairies. The Oceanic Niño Index has a moderate negative correlation with the smoothed interannual trends present in the HGS-derived TWSA; both time series have a prominent 2.7-3.0-year period signal shown in the Lomb-Scargle periodograms. Interannual trends in TWSA in the SSRB may be impacted as the characteristics and timing of El Niño events change with a changing climate.

https://doi.org/10.5194/egusphere-2025-3522
Preprint. Discussion started: 14 October 2025

Accurate, high-resolution observations and models are crucial to understanding the impact of climate change on the quantity of surface and groundwater in the SSRB. Comparing satellite measurements to high-resolution hydrological models provides a method of independent calibration and validation. The HGS model differs from GRACE-derived TWSA in seasonal amplitude and long-term trends but reproduces the interannual trends observed by GRACE/GRACE-FO and can be used to examine different components of water storage and their relationships to oceanic and meteorological forcing conditions. As extreme meteorological events and long-term changes due to rising temperatures impact hydrology in Southern Alberta, a comprehensive characterization of water storage is imperative for sustainable water management critical for all anthropogenic and ecological activities (Wheater and Gober, 2013). Future work involves using the HydroGeoSphere platform to further assess TWSA in the different physiographic regions within the SSRB and to identify primary drivers of water storage change within these regions.

Data availability

The software and data created for the analysis are located in a repository that will be published upon acceptance of the article, and can be provided upon request.

Author contribution

The CRediT contributor roles are as follows:

SB: Conceptualization, Formal analysis, Methodology, Software, Visualization, Writing – original draft preparation.

SKF.: Conceptualization, Funding acquisition, Methodology, Resources, Supervision, Visualization, Writing – original draft preparation, Writing – review & editing.

GF: Conceptualization, Funding acquisition, Methodology, Supervision, Writing – review & editing.

JC: Conceptualization, Methodology, Resources, Data curation, Writing – original draft preparation, Writing – review & editing.

BX: Methodology, Formal analysis, Data curation, Visualization, Writing – review & editing

OK: Methodology, Formal analysis, Writing – review & editing

HE: Methodology, Formal analysis, Data curation, Writing – review & editing

BF: Methodology, Formal analysis, Writing – review & editing

ARE.: Methodology, Formal analysis, Writing – review & editing

AG: Methodology, Formal analysis, Writing – review & editing, Funding acquisition

Competing Interests

https://doi.org/10.5194/egusphere-2025-3522
Preprint. Discussion started: 14 October 2025

The authors declare that they have no conflict of interest.

Acknowledgements

This work was supported through an a MITACS Accelerate Grant IT43296 in collaboration with Aquanty Inc and Queen's University. The Alberta Federation of Agriculture provided an early version of the SSRB HydroGeoSphere model that was used herein.

References

Abelen, S., Seitz, F., Abarca-del-Rio, R., and Güntner, A.: Droughts and Floods in the La Plata Basin in Soil Moisture Data and GRACE, Remote Sensing, 7, 7324–7349, https://doi.org/10.3390/rs70607324, 2015.

Alberta Agriculture and Rural Development: Alberta Irrigation Management Model (AIMM) v.3.1.3 Help Manual, Edmonton, 2013.

Alberta Geological Survey: 3D Provincial Geological Framework Model of Alberta, version 2, Alberta Energy Regulator / Alberta Geological Survey, 2019.

Aquanty: HydroGeoSphere Reference Manual, Waterloo, ON, 2024.

Armour, K. C., Bitz, C. M., and Roe, G. H.: Time-Varying Climate Sensitivity from Regional Feedbacks, Journal of Climate, 26, 4518–4534, https://doi.org/10.1175/JCLI-D-12-00544.1, 2013.

Asong, Z. E., Wheater, H. S., Bonsal, B., Razavi, S., and Kurkute, S.: Historical drought patterns over Canada and their teleconnections with large-scale climate signals, Hydrology and Earth System Sciences, 22, 3105–3124, https://doi.org/10.5194/hess-22-3105-2018, 2018.

Berg, A. and Sheffield, J.: Climate Change and Drought: the Soil Moisture Perspective, Curr Clim Change Rep, 4, 180–191, https://doi.org/10.1007/s40641-018-0095-0, 2018.

Bonsal, B. and Regier, M.: Historical comparison of the 2001/2002 drought in the Canadian Prairies, Climate Research, 33, 229–242, https://doi.org/10.3354/cr033229, 2007.

Bonsal, B. R., Aider, R., Gachon, P., and Lapp, S.: An assessment of Canadian prairie drought: past, present, and future, Clim Dyn, 41, 501–516, https://doi.org/10.1007/s00382-012-1422-0, 2013.

Bringeland, S. and Fotopoulos, G.: Analysis of gap filling techniques for GRACE/GRACE-FO terrestrial water storage anomalies in Canada, Journal of Hydrology, 630, 130644, https://doi.org/10.1016/j.jhydrol.2024.130644, 2024.

Bringeland, S., Frey, S. K., Fotopoulos, G., Crowley, J., Xu, B., Khader, O., Eum, H., Farjad, B., Erler, A. R., and Gupta, A.: Investigating terrestrial water storage change in a western Canadian river basin with GRACE/GRACE-FO and fully-integrated groundwater – surface water modelling, Zenodo [data set], https://doi.org/10.5281/zenodo.15120774, 2025.

https://doi.org/10.5194/egusphere-2025-3522
Preprint. Discussion started: 14 October 2025

Chartrand, J. and Pausata, F. S. R.: Impacts of the North Atlantic Oscillation on winter precipitations and storm track variability in southeast Canada and the northeast United States, Weather and Climate Dynamics, 1, 731–744, https://doi.org/10.5194/wcd-1-731-2020, 2020.

Chen, J. L., Wilson, C. R., Tapley, B. D., Yang, Z. L., and Niu, G. Y.: 2005 drought event in the Amazon River basin as measured by GRACE and estimated by climate models, Journal of Geophysical Research: Solid Earth, 114, https://doi.org/10.1029/2008JB006056, 2009.

Crowley, J., Mitrovica, J., Bailey, R., Tamisiea, M., and Davis, J.: Water Storage Variations Within the Congo and Amazon Basins Inferred From GRACE Satellite Gravity Data, AGU Fall Meeting Abstracts, 2006.

Crowley, J. W. and Huang, J.: A least-squares method for estimating the correlated error of GRACE models, Geophysical Journal International, 221, 1736–1749, https://doi.org/10.1093/GJI/GGAA104, 2020.

Davis, J. L., Tamisiea, M. E., Elósegui, P., Mitrovica, J. X., and Hill, E. M.: A statistical filtering approach for Gravity Recovery and Climate Experiment (GRACE) gravity data, Journal of Geophysical Research: Solid Earth, 113, https://doi.org/10.1029/2007JB005043, 2008.

Davitt, A., Schumann, G., Forgotson, C., and McDonald, K. C.: The Utility of SMAP Soil Moisture and Freeze-Thaw Datasets as Precursors to Spring-Melt Flood Conditions: A Case Study in the Red River of the North Basin, IEEE Journal of Selected Topics in Applied Earth Observations and Remote Sensing, 12, 2848–2861, https://doi.org/10.1109/JSTARS.2019.2918947, 2019.

Dumanski, S., Pomeroy, J. W., and Westbrook, C. J.: Hydrological regime changes in a Canadian Prairie basin, Hydrological Processes, 29, 3893–3904, https://doi.org/10.1002/hyp.10567, 2015.

Erler, A. R., Frey, S. K., Khader, O., d'Orgeville, M., Park, Y.-J., Hwang, H.-T., Lapen, D. R., Peltier, W. R., and Sudicky, E. A.: Evaluating Climate Change Impacts on Soil Moisture and Groundwater Resources Within a Lake-Affected Region, Water Resources Research, 55, 8142–8163, https://doi.org/10.1029/2018WR023822, 2019.

Eum, H.-I. and Gupta, A.: Hybrid climate datasets from a climate data evaluation system and their impacts on hydrologic simulations for the Athabasca River basin in Canada, Hydrol. Earth Syst. Sci., 23, 5151–5173, https://doi.org/10.5194/hess-23-5151-2019, 2019.

Eum, H.-I., Dibike, Y., and Prowse, T.: Climate-induced alteration of hydrologic indicators in the Athabasca River Basin, Alberta, Canada, Journal of Hydrology, 544, 327–342, https://doi.org/10.1016/j.jhydrol.2016.11.034, 2017.

Famiglietti, J. S., Lo, M., Ho, S. L., Bethune, J., Anderson, K. J., Syed, T. H., Swenson, S. C., de Linage, C. R., and Rodell, M.: Satellites measure recent rates of groundwater depletion in California's Central Valley, Geophysical Research Letters, 38, https://doi.org/10.1029/2010GL046442, 2011.

Fatolazadeh, F. and Goïta, K.: Mapping terrestrial water storage changes in Canada using GRACE and GRACE-FO, Science of The Total Environment, 779, 146435, https://doi.org/10.1016/j.scitotenv.2021.146435, 2021.

https://doi.org/10.5194/egusphere-2025-3522
Preprint. Discussion started: 14 October 2025

Frey, S. K., Miller, K., Khader, O., Taylor, A., Morrison, D., Xu, X., Berg, S. J., Hwang, H.-T., Sudicky, E. A., and Lapen, D. R.: Evaluating landscape influences on hydrologic behavior with a fully-integrated groundwater – surface water model, Journal of Hydrology, 602, 126758, https://doi.org/10.1016/j.jhydrol.2021.126758, 2021.

Geological Survey of Canada: Surficial geology of Canada, Prelim., Surficial Data Model V.2.0 Conversion., Natural Resources Canada, https://doi.org/10.4095/295462, 2014.

Girotto, M., De Lannoy, G. J. M., Reichle, R. H., Rodell, M., Draper, C., Bhanja, S. N., and Mukherjee, A.: Benefits and pitfalls of GRACE data assimilation: A case study of terrestrial water storage depletion in India, Geophysical Research Letters, 44, 4107–4115, https://doi.org/10.1002/2017GL072994, 2017.

Hamdi, M., El Alem, A., and Goita, K.: Groundwater Storage Estimation in the Saskatchewan River Basin Using GRACE/GRACE-FO Gravimetric Data and Machine Learning, Atmosphere, 16, 50, https://doi.org/10.3390/atmos16010050, 2025.

He, Z., Shook, K., Spence, C., Pomeroy, J. W., and Whitfield, C.: Modelling the regional sensitivity of snowmelt, soil moisture, and streamflow generation to climate over the Canadian Prairies using a basin classification approach, Hydrology and Earth System Sciences, 27, 3525–3546, https://doi.org/10.5194/hess-27-3525-2023, 2023.

Huang, B., Thorne, P. W., Banzon, V. F., Boyer, T., Chepurin, G., Lawrimore, J. H., Menne, M. J., Smith, T. M., Vose, R. S., and Zhang, H.-M.: Extended Reconstructed Sea Surface Temperature, Version 5 (ERSSTv5): Upgrades, Validations, and Intercomparisons, https://doi.org/10.1175/JCLI-D-16-0836.1, 2017.

Humphrey, V., Gudmundsson, L., and Seneviratne, S. I.: Assessing Global Water Storage Variability from GRACE: Trends, Seasonal Cycle, Subseasonal Anomalies and Extremes, Surv Geophys, 37, 357–395, https://doi.org/10.1007/s10712-016-9367-1, 2016.

Hurrell, J. W. and Deser, C.: North Atlantic climate variability: The role of the North Atlantic Oscillation, Journal of Marine Systems, 79, 231–244, https://doi.org/10.1016/j.jmarsys.2009.11.002, 2010.

Hwang, H.-T., Park, Y.-J., Sudicky, E. A., and Forsyth, P. A.: A parallel computational framework to solve flow and transport in integrated surface–subsurface hydrologic systems, Environmental Modelling & Software, 61, 39–58, https://doi.org/10.1016/j.envsoft.2014.06.024, 2014.

Hwang, H.-T., Erler, A. R., Khader, O., Berg, S. J., Sudicky, E. A., and Jones, J. P.: Estimation of groundwater contributions to Athabasca River, Alberta, Canada, Journal of Hydrology: Regional Studies, 45, 101301, https://doi.org/10.1016/j.ejrh.2022.101301, 2023.

Kienzle, S. W.: A new temperature based method to separate rain and snow, Hydrological Processes, 22, 5067–5085, https://doi.org/10.1002/hyp.7131, 2008.

Landerer, F. W., Flechtner, F. M., Save, H., Webb, F. H., Bandikova, T., Bertiger, W. I., Bettadpur, S. V., Byun, S. H., Dahle, C., Dobslaw, H., Fahnestock, E., Harvey, N., Kang, Z., Kruizinga, G. L. H., Loomis, B. D., McCullough, C., Murböck, M., Nagel, P., Paik, M., Pie, N., Poole, S., Strekalov, D., Tamisiea, M. E., Wang, F., Watkins, M. M., Wen, H.-Y., Wiese, D. N.,

https://doi.org/10.5194/egusphere-2025-3522
Preprint. Discussion started: 14 October 2025

and Yuan, D.-N.: Extending the Global Mass Change Data Record: GRACE Follow-On Instrument and Science Data Performance, Geophysical Research Letters, 47, e2020GL088306, https://doi.org/10.1029/2020GL088306, 2020.

Latifovic, R., Homer, C., Ressl, R., Pouliot, D., Hossain, S. N., Colditz, R. R., Olthof, I., Giri, C., and Victoria, A.: North American Land-Change Monitoring System, in: Remote Sensing of Land Use and Land Cover: Principles and Applications, CRC Press, 303–322, 2012.

Li, B., Beaudoing, H., and Rodell, M.: GLDAS Catchment Land Surface Model L4 monthly 1.0 x 1.0 degree V2.1, https://doi.org/10.5067/FOUXNLXFAZNY, 2020.

Lilly, J. M. and Olhede, S. C.: Higher-Order Properties of Analytic Wavelets, IEEE Transactions on Signal Processing, 57, 146–160, https://doi.org/10.1109/TSP.2008.2007607, 2009.

Lilly, J. M. and Olhede, S. C.: Generalized Morse Wavelets as a Superfamily of Analytic Wavelets, IEEE Transactions on Signal Processing, 60, 6036–6041, https://doi.org/10.1109/TSP.2012.2210890, 2012.

Lomb, N. R.: Least-squares frequency analysis of unequally spaced data, Astrophys Space Sci, 39, 447–462, https://doi.org/10.1007/BF00648343, 1976.

Loomis, B. D., Rachlin, K. E., and Luthcke, S. B.: Improved Earth Oblateness Rate Reveals Increased Ice Sheet Losses and Mass-Driven Sea Level Rise, Geophysical Research Letters, 46, 6910–6917, https://doi.org/10.1029/2019GL082929, 2019.

Lu, Z., Schultze, A., Carré, M., Brierley, C., Hopcroft, P. O., Zhao, D., Zheng, M., Braconnot, P., Yin, Q., Jungclaus, J. H., Shi, X., Yang, H., and Zhang, Q.: Increased frequency of multi-year El Niño–Southern Oscillation events across the Holocene, Nat. Geosci., 1–7, https://doi.org/10.1038/s41561-025-01670-y, 2025.

Mantua, N. J. and Hare, S. R.: The Pacific Decadal Oscillation, Journal of Oceanography, 58, 35–44, https://doi.org/10.1023/A:1015820616384, 2002.

Martz, L. W., Bruneau, J., and J. Terry Rolfe: Climate Change and Water: SSRB (South Saskatchewan River Basin) Final Technical Report, https://doi.org/10.13140/RG.2.2.12833.76646, 2007.

Masson-Delmotte, V., P., Z., Pirani, A., Connors, S. L., Pean, C., Berger, S., Caud, N., Goldfarb, L., Gomis, M. I., Huang, M., Leitzell, K., Lonnoy, E., Matthews, J. B. R., Maycock, T. K., Waterfield, T., Yelekci, O., Yu, R., and Zhou, B.: IPCC, 2021: Climate Change 2021: The Physical Science Basis. Contribution of Working Group I to the Sixth Assessment Report of the Intergovernmental Panel on Climate Change, Cambridge University Press, 2021.

McCabe, G. J. and Dettinger, M. D.: Primary Modes and Predictability of Year-to-Year Snowpack Variations in the Western United States from Teleconnections with Pacific Ocean Climate, J. Hydrometeor, 3, 13–25, https://doi.org/10.1175/1525-7541(2002)003<0013:PMAPOY>2.0.CO;2, 2002.

Moriasi, D. N., Arnold, J. G., Van Liew, M. W., Bingner, R. L., Harmel, R. D., and Veith, T. L.: Model Evaluation Guidelines for Systematic Quantification of Accuracy in Watershed Simulations, Transactions of the ASABE, 50, 885–900, https://doi.org/10.13031/2013.23153, 2007.

https://doi.org/10.5194/egusphere-2025-3522
Preprint. Discussion started: 14 October 2025

Newman, M., Alexander, M. A., Ault, T. R., Cobb, K. M., Deser, C., Di Lorenzo, E., Mantua, N. J., Miller, A. J., Minobe, S., Nakamura, H., Schneider, N., Vimont, D. J., Phillips, A. S., Scott, J. D., and Smith, C. A.: The Pacific Decadal Oscillation, Revisited, Journal of Climate, 29, 4399–4427, https://doi.org/10.1175/JCLI-D-15-0508.1, 2016.

NOAA (National Oceanic and Atmospheric Administration): Cold and warm episodes by season, 2019.

Peltier, W. R., Argus, D. F., and Drummond, R.: Space geodesy constrains ice age terminal deglaciation: The global ICE-6G_C (VM5a) model, Journal of Geophysical Research: Solid Earth, 120, 450–487, https://doi.org/10.1002/2014JB011176, 2015.

Peltier, W. R., Argus, D. F., and Drummond, R.: Comment on "An Assessment of the ICE-6G_C (VM5a) Glacial Isostatic Adjustment Model" by Purcell et al., Journal of Geophysical Research: Solid Earth, 123, 2019–2028, https://doi.org/10.1002/2016JB013844, 2018.

Pomeroy, J. W., Stewart, R. E., and Whitfield, P. H.: The 2013 flood event in the South Saskatchewan and Elk River basins: Causes, assessment and damages, Canadian Water Resources Journal / Revue canadienne des ressources hydriques, 41, 105–117, https://doi.org/10.1080/07011784.2015.1089190, 2016.

Rodell, M., Houser, P. R., Jambor, U., Gottschalck, J., Mitchell, K., Meng, C.-J., Arsenault, K., Cosgrove, B., Radakovich, J., Bosilovich, M., Entin, J. K., Walker, J. P., Lohmann, D., and Toll, D.: The Global Land Data Assimilation System, Bull. Amer. Meteor. Soc., 85, 381–394, https://doi.org/10.1175/BAMS-85-3-381, 2004.

Roderick, M. L., Greve, P., and Farquhar, G. D.: On the assessment of aridity with changes in atmospheric CO2, Water Resources Research, 51, 5450–5463, https://doi.org/10.1002/2015WR017031, 2015.

Sauchyn, D., Davidson, D., and Johnston, M.: Chapter 4: Prairie Provinces, in: Canada in a Changing Climate: Regional Perspectives Report, (ed) F.J. Warren, N. Lulham, and D. S. Lemmen, Government of Canada, 2020.

Save, H.: CSR GRACE and GRACE-FO RL06 Mascon Solutions v02 Available: http://www2.csr.utexas.edu/grace, https://doi.org/10.15781/cgq9-nh24, 2020.

Save, H., Bettadpur, S., and Tapley, B. D.: High-resolution CSR GRACE RL05 mascons, Journal of Geophysical Research: Solid Earth, 121, 7547–7569, https://doi.org/10.1002/2016JB013007, 2016.

Scanlon, B. R., Zhang, Z., Save, H., Sun, A. Y., Schmied, H. M., Beek, L. P. H. van, Wiese, D. N., Wada, Y., Long, D., Reedy, R. C., Longuevergne, L., Döll, P., and Bierkens, M. F. P.: Global models underestimate large decadal declining and rising water storage trends relative to GRACE satellite data, PNAS, 115, E1080–E1089, https://doi.org/10.1073/pnas.1704665115, 2018.

Scanlon, B. R., Rateb, A., Pool, D. R., Sanford, W., Save, H., Sun, A., Long, D., and Fuchs, B.: Effects of climate and irrigation on GRACE-based estimates of water storage changes in major US aquifers, Environ. Res. Lett., 16, 094009, https://doi.org/10.1088/1748-9326/ac16ff, 2021.

Scargle, J. D.: Studies in astronomical time series analysis. II. Statistical aspects of spectral analysis of unevenly spaced data., The Astrophysical Journal, 263, 835–853, https://doi.org/10.1086/160554, 1982.

https://doi.org/10.5194/egusphere-2025-3522
Preprint. Discussion started: 14 October 2025

Shabbar, A., Bonsal, B. R., and Szeto, K.: Atmospheric and Oceanic Variability Associated with Growing Season Droughts and Pluvials on the Canadian Prairies, Atmosphere-Ocean, 49, 339–355, https://doi.org/10.1080/07055900.2011.564908, 2011.

Soil Landscapes of Canada Working Group: Soil Landscapes of Canada version 3.2. Agriculture and Agri-Food Canada. (digital map and database at 1:1 million scale)., 2010.

Spence, C., He, Z., Shook, K. R., Mekonnen, B. A., Pomeroy, J. W., Whitfield, C. J., and Wolfe, J. D.: Assessing hydrological sensitivity of grassland basins in the Canadian Prairies to climate using a basin classification-based virtual modelling approach, Hydrology and Earth System Sciences, 26, 1801–1819, https://doi.org/10.5194/hess-26-1801-2022, 2022.

Sun, Y., Riva, R., and Ditmar, P.: Optimizing estimates of annual variations and trends in geocenter motion and J2 from a combination of GRACE data and geophysical models, Journal of Geophysical Research: Solid Earth, 121, 8352–8370, https://doi.org/10.1002/2016JB013073, 2016.

Swenson, S., Chambers, D., and Wahr, J.: Estimating geocenter variations from a combination of GRACE and ocean model output, Journal of Geophysical Research: Solid Earth, 113, https://doi.org/10.1029/2007JB005338, 2008.

Tangdamrongsub, N., Hwang, C., Borak, J. S., Prabnakorn, S., and Han, J.: Optimizing GRACE/GRACE-FO data and a priori hydrological knowledge for improved global terrestrial water storage component estimates, Journal of Hydrology, 598, 126463, https://doi.org/10.1016/j.jhydrol.2021.126463, 2021.

Tanzeeba, S. and Gan, T. Y.: Potential impact of climate change on the water availability of South Saskatchewan River Basin, Climatic Change, 112, 355–386, https://doi.org/10.1007/s10584-011-0221-7, 2012.

Tapley, B. D., Watkins, M. M., Flechtner, F., Reigber, C., Bettadpur, S., Rodell, M., Sasgen, I., Famiglietti, J. S., Landerer, F. W., Chambers, D. P., Reager, J. T., Gardner, A. S., Save, H., Ivins, E. R., Swenson, S. C., Boening, C., Dahle, C., Wiese, D. N., Dobslaw, H., Tamisiea, M. E., and Velicogna, I.: Contributions of GRACE to understanding climate change, Nat. Clim. Chang., 9, 358–369, https://doi.org/10.1038/s41558-019-0456-2, 2019.

Veeman, T. and Veeman, M.: Agriculture and Food, The Canadian Encyclopedia, 2015.

Wahr, J., Molenaar, M., and Bryan, F.: Time variability of the Earth's gravity field: Hydrological and oceanic effects and their possible detection using GRACE, Journal of Geophysical Research: Solid Earth, 103, 30205–30229, https://doi.org/10.1029/98JB02844, 1998.

Walter, M. T., Brooks, E. S., McCool, D. K., King, L. G., Molnau, M., and Boll, J.: Process-based snowmelt modeling: does it require more input data than temperature-index modeling?, Journal of Hydrology, 300, 65–75, https://doi.org/10.1016/j.jhydrol.2004.05.002, 2005.

Watkins, M. M., Wiese, D. N., Yuan, D.-N., Boening, C., and Landerer, F. W.: Improved methods for observing Earth's time variable mass distribution with GRACE using spherical cap mascons, Journal of Geophysical Research: Solid Earth, 120, 2648–2671, https://doi.org/10.1002/2014JB011547, 2015.

Wheater, H. and Gober, P.: Water security in the Canadian Prairies: science and management challenges, Phil. Trans. R. Soc. A., 371, 20120409, https://doi.org/10.1098/rsta.2012.0409, 2013.

https://doi.org/10.5194/egusphere-2025-3522
Preprint. Discussion started: 14 October 2025

Wiese, D. N., Landerer, F. W., and Watkins, M. M.: Quantifying and reducing leakage errors in the JPL RL05M GRACE mascon solution, Water Resources Research, 52, 7490–7502, https://doi.org/10.1002/2016WR019344, 2016.

Wiese, D. N., Yuan, D.-N., Boening, C., Landerer, F. W., and Watkins, M. M.: JPL GRACE and GRACE-FO Mascon Ocean, Ice, and Hydrology Equivalent Water Height Coastal Resolution Improvement (CRI) Filtered Release 06.1 Version 03 Available: http://grace.jpl.nasa.gov, https://doi.org/10.5067/TEMSC-3JC63, 2023.

Wittrock, V. and Ripley, E. a.: The predictability of autumn soil moisture levels on the Canadian Prairies, International Journal of Climatology, 19, 271–289, https://doi.org/10.1002/(SICI)1097-0088(19990315)19:3<271::AID-JOC362>3.0.CO;2-G, 1999.

Yeh, S.-W., Kug, J.-S., Dewitte, B., Kwon, M.-H., Kirtman, B. P., and Jin, F.-F.: El Niño in a changing climate, Nature, 461, 511–514, https://doi.org/10.1038/nature08316, 2009.

Zhang, Z., Li, Y., Barlage, M., Chen, F., Miguez-Macho, G., Ireson, A., and Li, Z.: Modeling groundwater responses to climate change in the Prairie Pothole Region, Hydrology and Earth System Sciences, 24, 655–672, https://doi.org/10.5194/hess-24-655-2020, 2020.